Additive Phenotypes Underlie Epistasis of Fitness Effects

Andrew M. Sackman and Darin R. Rokyta[1]
Department of Biological Science, Florida State University, Tallahassee, Florida 32306

ABSTRACT Gene interactions, or epistasis, play a large role in determining evolutionary outcomes. The ruggedness of fitness landscapes, and thus the predictability of evolution and the accessibility of high-fitness genotypes, is determined largely by the pervasiveness of epistasis and the degree of correlation between similar genotypes. We created all possible pairings of three sets of five beneficial first-step mutations fixed during adaptive walks under three different regimes: selection on growth rate alone, on growth rate and thermal stability, and on growth rate and pH stability. All 30 double-mutants displayed negative, antagonistic epistasis with regard to growth rate and fitness, but positive epistasis and additivity were common for the stability phenotypes. This suggested that biophysically simple phenotypes, such as capsid stability, may on average behave more additively than complex phenotypes like viral growth rate. Growth rate epistasis was also smaller in magnitude when the individual effects of single mutations were smaller. Significant sign epistasis, such that the effect of a mutation that is beneficial in the wild-type background is deleterious in combination with a second mutation, emerged more frequently in intragenic mutational pairings than in intergenic pairs, and was evident in nearly half of the double-mutants, indicating that the fitness landscape is moderately uncorrelated and of intermediate ruggedness. Together, our results indicated that mutations may interact additively with regard to phenotype when considered at a basic, biophysical level, but that epistasis arises as a result of pleiotropic interactions between the individual components of complex phenotypes and diminishing returns arising from intermediate phenotypic optima.

KEYWORDS epistasis; pleiotropy; experimental evolution; capsid stability

THE evolutionary fate of an adapting population is largely determined by the shape of its adaptive landscape (Wright 1932, 1988). A smooth landscape featuring continuous ascents toward a universal adaptive peak will invariably lead a population along a deterministic path toward the optimum. Rugged landscapes with many local peaks and valleys result in unpredictable adaptive walks and potentially suboptimal fitness (Wright 1932; Kauffman and Levin 1987; Whitlock *et al.* 1995). Epistasis, or interactions between genes or loci, is the primary determinant of the ruggedness or smoothness of fitness landscapes, and thus the accessibility of high-fitness genotypes and the pace and predictability of adaptation (Kvitek and Sherlock 2011).

Many forms of epistasis have been demonstrated empirically in a variety of systems, including examples of both negative epistasis (Elena and Lenski 1997; Sanjuán *et al.* 2004; Rokyta *et al.* 2011; Caudle *et al.* 2014; Bank *et al.* 2015; Ono *et al.* 2017; Zee and Velicer 2017), such that the effect of multiple mutations in combination is less than the sum of their individual effects, and positive epistasis (de Visser *et al.* 1997; Pepin and Wichman 2007; Vanhaeren *et al.* 2014), such that the effect of multiple mutations in combination exceeds the sum of their individual effects. Additionally, sign epistasis, where the sign of the effect of a mutation is dependent upon its genetic context, has also been frequently observed (Elena and Lenski 1997; Rokyta *et al.* 2002; Poon and Chao 2005; Weinreich *et al.* 2005; Breen *et al.* 2012; Sackman and Rokyta 2013; Caudle *et al.* 2014; Sackman *et al.* 2015; Ono *et al.* 2017). Despite the importance of epistasis in determining evolutionary outcomes, the mechanisms underlying epistasis are elusive and our ability to predict interactions remains incomplete due to the complexity of epistatic patterns and limitations of experimental methods (Poon and Chao 2006; Martin *et al.* 2007; Lehner 2011; Draghi and Plotkin 2013; Bank *et al.* 2016).

To explore patterns of epistatic interactions between beneficial mutations, we constructed 30 double-mutant genotypes from a common wild-type bacteriophage background and pairs of individual beneficial single-step mutations. Our experiment differed from previous attempts to characterize

doi: https://doi.org/10.1534/genetics.117.300451
Manuscript received August 9, 2017; accepted for publication November 3, 2017; published Early Online November 7, 2017.
[1]Corresponding author: Department of Biological Science, Florida State University, 1319 Stadium Dr., Tallahassee, FL 32306-4295. E-mail: drokyta@bio.fsu.edu

epistasis between beneficial mutations in that our sets of single-step mutations were generated under three different types of experimental selection: selection acting on growth rate alone; selection acting on growth rate and on capsid stability during thermal shock; and selection acting on growth rate and on capsid stability during low-pH shock. Our measurements of fitness were thus decomposable into phenotypes, allowing us to test for epistasis for both fitness and individual phenotypes. Additionally, although the overall effect of each single mutation was beneficial, several mutations had deleterious effects on one of the two components of fitness (growth rate and decay rate), so rather than assessing interactions of strictly beneficial or strictly deleterious mutations as in many previous works (Elena and Lenski 1997; MacLean *et al.* 2010; Chou *et al.* 2011; Rokyta *et al.* 2011; Caudle *et al.* 2014), we measured phenotypic effects of combinations of both categories of mutations. We assayed fitness of the single- and double-mutants under their original selective regime, and calculated the sign and magnitude of epistasis on fitness and its individual components.

Materials and Methods

Bacteriophage ancestor

The ID8 microvirid genotype was originally isolated by Rokyta *et al.* (2006) (GenBank accession number DQ079898). ID8 is a single-stranded DNA bacteriophage with a genome length of 5540 nt encoding 11 genes.

Generation of single-step beneficial mutations

The mutations used to construct the libraries of double-mutants were originally generated by McGee *et al.* (2016). Twenty replicate first adaptive steps were performed from unique isolates of wild-type ID8 under three different types of selection: growth-only selection, selection on both growth rate and thermal stability, and selection on growth rate and pH stability. Experimental evolution was performed through serial passaging in orbital shaking water baths at 37° and 200 rpm in 10 ml of lysogeny broth. Approximately 10^5 phage were added to $\sim 10^8$ *Escherichia coli* hosts and grown for either 40 or 60 min, depending on the selective regime. Growth was terminated with $CHCl_3$, the resulting sample was centrifuged, and a fraction of the supernatant was used to initiate the next passage.

Growth-rate mutations were generated by subjecting adapting populations only to selection acting on growth rate through this standard passaging protocol with a 40-min growth period. Heat-shock mutations were generated by extending the growth period to 60 min and adding a 12-min heat-shock period between each growth passage. Following the addition of $CHCl_3$ and centrifugation, 1 ml of phage-laden supernatant was split between two 0.65-ml microcentrifuge tubes and submerged in an ice bath for 5 min to normalize the sample temperature, then submerged in hot beads at 80° for 12 min. Samples were returned to the ice bath for 5 min and then used to initiate the next growth passage.

pH mutations were generated by following each 60-min growth period with a 3-min pH shock. The pH of 1 ml of sample was lowered to 1.5 with 0.5 M HCl for 3 min and then raised back to pH 7 with 0.5 M NaOH. Population sizes were monitored by plating on agar plates at three points for each growth–death cycle: initial concentration prior to growth, concentration after growth, and concentration after heat shock. Population change rates were calculated on a log2 scale resulting in values of population doublings/halvings per hour.

Only the 12-min heat-shock mutations from McGee *et al.* (2016) were used for this experiment, as the 5-min heat-shock mutations had significantly smaller effects on stability and were not likely to be of interest in this experiment. For additional details on methods and the single-step mutations, see McGee *et al.* (2016).

Construction of double-mutant libraries

Five mutations were randomly chosen from each of the sets of growth-rate, heat-shock, and pH-shock mutations described by McGee *et al.* (2016). Only mutations affecting genes for which full protein structures are available were considered, limiting us to mutations affecting the coat protein (F) and spike protein (G). This was done to allow for future application of the molecular-dynamics simulation method described by McGee *et al.* (2014) to estimate the changes in capsid stability induced by the selected mutations. Additionally, the heat- and pH shocks acted only on mature viral capsids in the absence of live hosts, and therefore our biophysical selective pressure only acted on variation in capsid genes. F and G therefore have at least the potential for contributing to variation in both growth rate and stability. One of the growth-selection mutations randomly selected for this experiment also appeared in the set of five randomly chosen pH-stability mutations.

All possible combinations within each set of five growth, heat-shock, and pH-shock mutations were generated via site-directed mutagenesis (Pepin *et al.* 2006; Pepin and Wichman 2007; Sackman and Rokyta 2013; Sackman *et al.* 2015). For each pair of mutations, a pair of primers centered on the first mutation and containing the derived base state were used in a pair of reactions with phage that had been sequence confirmed to contain the second mutation, with no additional changes to the ancestral genotype. These reactions produced two amplified genome fragments overlapping at the mutation site and at a region located on the opposite end of the circular genome. The amplified genome fragments were combined in a PCR without primers to assemble complete genome copies containing both desired mutations, and the products were purified, electroporated, isolated, and confirmed to be free of additional mutations by full-genome Sanger sequencing.

Electroporation of most double-mutant genomes successfully produced error-free isolates on the first attempt. All double-mutants were successfully built within three attempts, with the exception of two heat-shock pairs: FG (F248/F355) and HJ (G38/G168). These two pairs were attempted no fewer

Table 1 Summary of single-step mutants used for construction of double-mutants

Label	Selection condition	Protein function	Protein name	Aa position	ΔAa	Nuc. position	ΔNuc.
A	Growth	Capsid	F	340	A → V	3587	C → T
B		Spike	G	10	N → S	4011	A → G
C		Spike	G	171	T → A	4493	A → G
D		Spike	G	171	T → I	4494	C → T
E		Spike	G	172	V → I	4496	G → A
F	Growth + heat-shock	Capsid	F	249	V → I	3310	G → A
G		Capsid	F	355	P → S	3628	C → T
H		Spike	G	38	R → C	4094	C → T
I		Spike	G	168	R → C	4484	C → T
K	Growth + pH shock	Capsid	F	77	I → T	2792	T → C
L		Capsid	F	393	I → V	3742	A → G
M		Spike	G	65	T → A	4175	A → G
N		Spike	G	69	N → S	4188	A → G
O		Spike	G	171	T → A	4493	A → G

Aa, amino acid; Nuc., nucleotide.

than 10 times each under a range of PCR parameters, as well as at a variety of incubation temperatures, to determine whether mutagenesis resulted in viable phages that were merely temperature sensitive, and never succeeded in producing a plaque following electroporation. Thus, we consider these two pairs of mutations to be lethal in combination in the ID8 wild-type background.

Fitness assays

Fitness assays were performed as described by McGee *et al.* (2016). Five replicate passages were initiated with $\sim 10^4$ phage of each sequence-confirmed isolate, with passage parameters identical to those described above for each selective regime. Wild-type ID8 was assayed independently with unique isolates under each selective regime, resulting in slightly different growth-rate values for ID8 within each set of 10 double-mutants.

Each assay population was plated to determine the concentrations of the isolate before growth, the population following the growth period, and the heat- or pH-shocked population. Growth rate (γ) was determined by calculating the population change rates on a $\log_2$ scale, resulting in a measurement of population doublings per hour. Decay rate (δ) was calculated as $\log_2$ population halvings per hour. Fitness, w, was calculated as $w = \gamma\tau_g + \delta\tau_d$, where τ_g and τ_d are equal to the time spent in the growth period and shock period, respectively.

Statistical analyses

Pairwise comparisons and sequential Bonferroni corrections were used to determine growth rate, decay rate, and fitness between double-mutants and the single-mutants and wild-type. All statistical analyses were performed using R (R Development Core Team 2010).

Data availability

Strains are available upon request. The sequence of our ancestral strain ID8 is available in GenBank under accession number DQ079898, and all mutations of ID8 used in this experiment are described in Table 1.

Results and Discussion

Antagonistic epistasis is universal for growth rate and fitness

We generated all 10 possible pairings for each of three sets of five randomly chosen first-step adaptive mutations generated on a wild-type microvirid bacteriophage background, ID8, under three different selective regimes (Table 1). The first set of mutations fixed under selection acting only on the phenotype of viral growth rate. For these mutations, fitness was measured as the $\log_2$ increase in population size over a 40-min growth period (see *Materials and Methods*), estimated as the average difference between viral titers at the ends and starts of at least five replicate assay passages. The second and third sets of first-step mutations arose under alternating selection on growth rate and a second biophysical phenotype, stability during high thermal shock and stability during low-pH shock, respectively. For these second and third sets of mutations, fitness (w) was decomposable into measurements of the two traits under selection: the phenotypes of growth rate and stability. Fitness was again measured as the average difference between the viral titers at the ends and starts of at least five replicate passages, equivalent to the average of the phenotypes of growth rate (γ) and stability, or decay rate (δ), weighted by the time spent in each phase during experimental passaging (τ_g and τ_d) (McGee *et al.* 2016). Fitness was therefore measured as

$$w = \gamma\tau_g + \delta\tau_d. \quad (1)$$

This definition of fitness also applies to the growth-selection mutants, with the time spent in the decay phase being zero. We defined epistasis as a deviation from the expected additivity of mutational effects. Because our fitness was measured as a rate of population doublings or halvings per hour, the expectation

under additivity is that the effect of two mutations in combination should be the sum of the effects of each individual mutation. We used a Malthusian measurement of fitness as a continuous growth rate on a log scale, so an additive expectation of nonepistatic interaction between mutations was therefore appropriate, rather than a multiplicative null expectation. The deviation from additivity can then be measured as

$$\epsilon_{ij} = \Delta w_{ij} - (\Delta w_i + \Delta w_j), \quad (2)$$

where Δw_{ij} is the effect of the double-mutant with mutations i and j relative to the wild-type, and Δw_i and Δw_j are the effects of the single-mutants i and j relative to the wild-type (Rokyta *et al.* 2011). An ϵ of 0 indicated additivity of effects. Positive epistasis was indicated by $\epsilon > 0$, such that the effect of the two mutations in combination was larger than expected under additivity. Negative epistasis was indicated by $\epsilon < 0$, or that the effect of the mutations together in the same background was less than expected. The terms synergistic and antagonistic epistasis have been used before with sets of only beneficial or only deleterious mutations to refer to positive and negative epistasis (Rokyta *et al.* 2011). However, while all single-step growth mutants were beneficial, and all stability mutants were beneficial at the level of fitness, several stability single-step mutants were deleterious to some extent for either growth rate or decay rate, complicating the use of the terms of antagonistic and synergistic epistasis. If observed and expected effects were both positive and $\epsilon > 0$, or if observed and expected effects were both negative and $\epsilon < 0$, epistasis was synergistic. In all other instances, including cases for which the signs of Δw_{ij} and $\Delta w_i + \Delta w_j$ differ, epistasis was antagonistic (Caudle *et al.* 2014). The fitnesses of the wild-type, single mutations, and double-mutants for the growth-only, growth rate and heat stability, and growth rate and pH stability sets are detailed in Table 2, Table 3, and Table 4, respectively. Each individual mutation was assigned a letter label (Table 1), and each double-mutant was labeled as a combination of the labels for each of its two single-step mutations.

Epistasis was negative and antagonistic with regard to fitness for all 30 double-mutants and for the growth-rate phenotype of all 20 stability mutations (Figure 1). Growth rate epistasis, $\epsilon\gamma_{ij}$, was negative for all 20 pairs of stability mutations, implying that growth rate was lower than expected under additivity across all pairings. For growth rate for the heat stability double-mutants $\overline{\epsilon\gamma_{ij}}$ was -2.68, and it was -4.85 for the pH stability double-mutants. $\overline{\epsilon_{ij}}$ was -7.23, -3.60, and -4.63 doublings per passage for the growth, heat, and pH double-mutants, respectively. An extreme form of negative epistasis manifested in the double-mutant combinations FG and HJ. After at least 10 attempts to generate viable double-mutant genotypes and exploration of alternative permissive culturing conditions, both of these mutant combinations failed to produce viable phage and were assumed to be lethal.

Our results for growth rate and fitness were largely in agreement with previous experimental characterizations of epistasis, particularly in viral systems, which have generally found a majority of interactions between beneficial mutations to be antagonistic in nature (Sanjuán *et al.* 2004; Rokyta *et al.* 2011; Caudle *et al.* 2014; Bank *et al.* 2015). However, the results are unique insofar as no examples of additivity or positive epistasis were observed, as most experiments finding a predominance of antagonistic epistasis have generally found a mix of antagonistic and synergistic or positive interactions (Pepin and Wichman 2007; Khan *et al.* 2011; Bank *et al.* 2015). Many studies have repeatedly demonstrated a deceleration in the rate of fitness increase of adapting populations over time (Lenski *et al.* 1991; Bull *et al.* 1997; de Visser and Lenski 2002; Elena and Lenski 2003; Khan *et al.* 2011; Vanhaeren *et al.* 2014), which may be largely attributable to antagonistic epistasis between beneficial mutations (Khan *et al.* 2011). A general trend toward antagonistic epistasis, not just in these phages but also in higher-level organisms that are subject to a twofold cost of sex, would also conflict with the mutational deterministic theory for the evolution of sex, which posits that sex provides an adaptive advantage when deleterious mutations interact synergistically. In this case, synergistic epistasis would allow populations to more effectively purge deleterious mutations (Otto and Feldman 1997; Kondrashov 1982, 1988, 1993; Otto 2009), though other theoretical work has shown that antagonistic epistasis may be favored in the presence of recombination, as a protective buffer against the effects of deleterious mutations (Desai *et al.* 2007).

Table 2 Summary of mutational effects for mutations evolved under growth selection

Strain	Fitness	Δw_{wt}	Δw_{add}	Δw_1	Δw_2	ϵw_{ij}
ID8	14.57 ± 0.32	—	—	—	—	—
A	18.16 ± 0.40	3.59	—	—	—	—
B	20.55 ± 0.46	5.98	—	—	—	—
C	20.42 ± 0.29	5.85	—	—	—	—
D	21.11 ± 0.14	6.54	—	—	—	—
E	20.97 ± 0.12	6.40	—	—	—	—
AB	19.49 ± 0.26	4.92	9.56	−1.05	1.33	−4.64
AC	19.26 ± 0.38	4.69	9.44	−1.16	1.10	−4.74
AD	20.05 ± 0.30	5.48	10.13	−1.06	1.89	−4.65
AE	19.92 ± 0.16	5.35	9.99	−1.05*	1.77	−4.64
BC	19.04 ± 0.31	4.47	11.83	−1.38	−1.51	−7.36
BD	17.58 ± 0.50	3.01	12.52	−3.54*	−2.97*	−9.52
BE	14.42 ± 0.19	−0.15	12.38	−6.56*	−6.13*	−12.53
CD	20.29 ± 0.40	5.72	12.39	−0.82	−0.13	−6.67
CE	18.44 ± 0.48	3.87	12.25	−2.53*	−1.97	−8.38
DE	18.34 ± 0.39	3.77	12.94	−2.63*	−2.77*	−9.17

Fitnesses are given as the average ± SE over five replicate fitness assay measurements. Δw_{wt} denotes the fitness effect of the genotype relative to the wild-type (ID8). Δw_{add} gives the expected fitness of a mutation pair under additivity. Δw_1 gives the effect of adding the first mutation in the double-mutant genotype name into the background of the second, and Δw_2 gives the effect of the second mutation in the background of the first. These are measurements of sign epistasis. ϵw_{ij} denotes the deviation from additivity, as calculated by Equation 2 or by subtracting the value of Δw_{add} from Δw_{wt}. A * denotes significant sign epistasis for $\Delta\gamma_1$ or $\Delta\gamma_2$.

Additivity and synergism in capsid stability

The sets of heat-shock and pH-shock double-mutants displayed a mix of positive and negative epistasis for decay rate, as well as several instances of additive effects (Figure 1B,

Table 3 Summary of mutational effects for mutations evolved under heat-shock selection

Strain	Growth rate (γ)	$\Delta\gamma_{wt}$	$\Delta\gamma_{add}$	$\Delta\gamma_1$	$\Delta\gamma_2$	$\epsilon_{\gamma ij}$	Decay rate (δ)	$\Delta\delta_{wt}$	$\Delta\delta_{add}$	$\Delta\delta_1$	$\Delta\delta_2$	$\epsilon_{\delta ij}$	Overall fitness (w)	Δw_{wt}	Δw_{add}	Δw_1	Δw_2	ϵ_{ij}
ID8	13.06 ± 0.22	—	—	—	—	—	−33.70 ± 1.49	—	—	—	—	—	6.32 ± 0.30	—	—	—	—	—
F	12.53 ± 0.17	−0.53	—	—	—	—	−22.13 ± 0.87	11.56	—	—	—	—	8.10 ± 0.18	1.79	—	—	—	—
G	15.53 ± 0.10	2.48	—	—	—	—	−25.49 ± 0.83	8.21	—	—	—	—	10.44 ± 0.24	4.12	—	—	—	—
H	16.12 ± 0.17	3.06	—	—	—	—	−25.00 ± 1.61	8.70	—	—	—	—	11.12 ± 0.26	4.80	—	—	—	—
I	18.03 ± 0.25	4.98	—	—	—	—	−48.16 ± 1.93	−14.46	—	—	—	—	8.40 ± 0.16	2.09	—	—	—	—
J	15.24 ± 0.17	2.18	—	—	—	—	−22.12 ± 0.96	11.58	—	—	—	—	10.82 ± 0.11	4.50	—	—	—	—
FG	Lethal	−13.06	2.53	—	—	−15.59	—	—	19.77	—	—	—	0	−6.32	5.91	—	—	−12.23
FH	13.50 ± 0.30	0.45	2.53	−2.62	0.97	−2.09	−28.55 ± 1.32	5.15	20.26	−3.55	−6.42*	−15.12	7.79 ± 0.20	1.47	6.59	−3.33*	−0.31	−5.11
FI	15.62 ± 0.28	2.56	4.45	−2.41	3.09	−1.89	−32.86 ± 1.45	0.83	−2.90	15.29	−10.73	3.73	9.05 ± 0.26	2.73	3.87	0.65	0.95	−1.14
FJ	13.03 ± 0.47	−0.02	1.66	−2.21	0.50	−1.68	−24.24 ± 1.10	9.46	23.14	−2.12	−2.11	−13.69	8.19 ± 0.27	1.87	6.28	−2.63*	0.08	−4.42
GH	17.27 ± 0.13	4.21	5.54	1.15	1.73	−1.33	−27.98 ± 1.19	5.72	16.90	−2.97	−2.48	−11.18	11.67 ± 0.23	5.36	8.92	0.56	1.24	−3.56
GI	18.32 ± 0.43	5.26	7.45	0.29	2.79	−2.19	−37.38 ± 1.69	−3.68	−6.25	10.78	−11.88	2.58	10.85 ± 0.28	4.53	6.20	2.44	0.41	−1.68
GJ	16.26 ± 0.19	3.20	4.66	1.02	0.72	−1.46	−21.54 ± 1.32	12.16	19.78	0.59	3.96	−7.62	11.95 ± 0.30	5.63	8.62	1.14	1.52	−2.98
HI	14.89 ± 0.45	1.84	8.04	−3.14*	−1.23	−6.20	−34.69 ± 1.27	−0.99	−5.76	13.47	−9.68	4.78	7.96 ± 0.23	1.64	6.89	−0.45	−3.16*	−5.25
HJ	Lethal	−13.06	5.24	—	—	−18.30	—	—	20.28	—	—	—	0	−6.32	9.30	—	—	−15.62
IJ	15.58 ± 0.30	2.53	7.16	0.34	−2.45*	−4.63	−36.61 ± 0.51	−2.91	−2.89	−14.48	11.55	−0.02	8.26 ± 0.23	1.95	6.58	−2.55*	−0.14	−4.64

γ, δ, and w are given as the average ± SE over five replicate fitness assay measurements. $\Delta\gamma_{wt}$, $\Delta\delta_{wt}$, and Δw_{wt} denote the fitness effect of the genotype relative to the wild-type (ID8). $\Delta\gamma_{add}$, $\Delta\delta_{ad}$, and Δw_{add} give the expected fitness of a mutation pair under additivity. $\Delta\gamma_1$, $\Delta\delta_1$, and Δw_1 give the effect of adding the first mutation in the double-mutant genotype name into the background of the second, and $\Delta\gamma_2$, $\Delta\delta_2$, and Δw_2 give the effect of the second mutation in the background of the first. These are measurements of sign epistasis. $\epsilon\gamma_{ij}$, $\epsilon\delta_{ij}$, and ϵ_{ij} denote the deviation from additivity, as calculated by Equation 2 or by subtracting the value of $\Delta\gamma_{add}$, $\Delta\delta_{add}$, or Δw_{add} from $\Delta\gamma_{wt}$, $\Delta\delta_{wt}$, or Δw_{wt}. A * for each double-mutant denotes significant sign epistasis for the effects of each single mutation in the background containing the second single mutation.

Table 3, and Table 4). Decay rate in the heat stability mutants showed an overall trend of negative epistasis (mean value of epistasis for decay rate, $\overline{\epsilon\delta_{ij}} = -4.57$, excluding lethal mutations), but three of the eight nonlethal double-mutants—FI, GI, and HI—showed positive epistasis, and one pairing, IJ, was additive. Epistasis for decay rate in the pH stability mutants was positive on average ($\overline{\epsilon\delta_{ij}} = 4.37$) and was only significantly negative for three of the ten pairings (LN, LO, and NO). Epistasis was synergistic for three pH double-mutants, LM, LO, and NO. The average magnitude of epistasis was not significantly different from the additive expectation of $\overline{\epsilon\delta_{ij}} = 0$ (Welch's two-sample t-tests; $P = 0.16$ for heat-shock mutants and $P = 0.54$ for pH mutants), so we could not reject the null expectation of additivity of stability effects.

These observations of positive and synergistic epistasis were unexpected given the preponderance of empirical data in this system indicating a general trend of antagonistic and negative epistasis (Rokyta *et al.* 2011; Caudle *et al.* 2014). All double-mutants in our experiment showed strong negative epistasis for growth rate and fitness. However, contrary to prior results, our double-mutants showed frequent positive epistasis for the phenotype of decay rate. This is further seen in the average measurement of ϵ relative to the average single-mutant effect size, $\overline{|\epsilon|}/\overline{|\Delta w_{wt}|}$, which was 1.21 and 1.13 when averaged over all growth effects and all fitness effects, respectively. The average epistatic effect observed for decay effects, 0.52, was less than half that observed for growth and fitness effects.

A possible explanation for these results lies in the root causes of epistasis. Capsid stability is a simple biophysical phenotype, with variation in stability arising from differences in the binding affinities between the constituent protein subunits of the capsid structure, and a mutation's biophysical effect on stability should be largely independent of other sites (DePristo *et al.* 2005). Effects of mutations on stability, or decay rate, may therefore act more additively than effects on growth rate and fitness, which are derived from complex assembly processes. Theoretical work has demonstrated that stabilizing selection resulting from pleiotropy generates epistasis for fitness due to a nonlinear relationship between phenotype and fitness, even when mutations act additively with regard to phenotype (Martin *et al.* 2007; de Visser *et al.* 2011; Chiu *et al.* 2012). Pleiotropy inherent to fitness and to the complex phenotype of growth rate, which is actually a composite phenotype encapsulating the traits of assembly rate, attachment rate, and lysis time, increases the likelihood that pairs of mutations interfere with each other, leading to reduced effect sizes relative to additive expectations.

Our results suggested that effects may be additive with regard to the effect of genotype on phenotype when considered at their most basic, biophysical level. The average deviation from additivity was closer to zero for decay effects, but when we scaled up to higher levels of phenotypic complexity or to the level of fitness, effects deviated significantly from additive expectations. Our results concur with those of Wells (1990), DePristo *et al.* (2005), and Olson *et al.* (2014), who

Table 4 Summary of mutational effects for mutations evolved under pH-shock selection

Strain	Growth rate (γ)	$\Delta\gamma_{wt}$	$\Delta\gamma_{add}$	$\Delta\gamma_1$	$\Delta\gamma_2$	$\epsilon_{\gamma ij}$	Decay rate (δ)	$\Delta\delta_{wt}$	$\Delta\delta_{add}$	$\Delta\delta_1$	$\Delta\delta_2$	$\epsilon_{\delta ij}$	Overall fitness (w)	Δw_{wt}	Δw_{add}	Δw_1	Δw_2	ϵ_{ij}
ID8	13.72 ± 0.19	—	—	—	—	—	−123.50 ± 5.29	—	—	—	—	—	7.55 ± 0.16	—	—	—	—	—
K	18.08 ± 0.10	4.35	—	—	—	—	−139.44 ± 7.81	−15.94	—	—	—	—	11.11 ± 0.44	3.56	—	—	—	—
L	17.26 ± 0.14	3.54	—	—	—	—	−116.37 ± 7.33	7.13	—	—	—	—	11.44 ± 0.43	3.90	—	—	—	—
M	16.50 ± 0.27	2.77	—	—	—	—	−114.94 ± 4.34	8.56	—	—	—	—	10.75 ± 0.33	3.20	—	—	—	—
N	18.03 ± 0.18	4.31	—	—	—	—	−125.36 ± 6.17	−1.86	—	—	—	—	11.76 ± 0.42	4.21	—	—	—	—
O	18.27 ± 0.06	4.54	—	—	—	—	−126.80 ± 5.72	−3.29	—	—	—	—	11.93 ± 0.28	4.38	—	—	—	—
KL	16.15 ± 0.30	2.43	7.89	−1.11	−1.93*	−5.46	−92.10 ± 8.53	31.40	−8.81	24.27	47.34	40.22	11.55 ± 0.46	4.00	7.45	0.10	0.44	−3.45
KM	17.32 ± 0.34	3.60	7.13	0.83	−0.75	−3.53	−118.58 ± 11.14	4.92	−7.38	−3.64	20.86	12.30	11.39 ± 0.32	3.85	6.76	0.65	0.29	−2.91
KN	18.90 ± 0.30	5.18	8.66	0.87	0.82	−3.48	−127.90 ± 5.01	−4.39	−17.80	−2.54	11.55	13.41	12.50 ± 0.29	4.96	7.77	0.74	1.40	−2.81
KO	17.80 ± 0.33	4.08	8.90	−0.47	−0.28	−4.82	−121.22 ± 7.44	2.28	−19.24	5.57	18.22	21.51	11.74 ± 0.33	4.19	7.93	−0.19	0.63	−3.74
LM	16.76 ± 0.33	3.04	6.31	0.27	−0.50	−3.27	−95.41 ± 5.18	28.09	15.69	19.53	20.96	12.40	11.99 ± 0.39	4.44	7.10	1.24	0.55	−2.65
LN	16.85 ± 0.29	3.12	7.85	−1.18	−0.41	−4.72	−124.34 ± 8.23	−0.84	5.27	1.02	−7.97	−6.11	10.63 ± 0.45	3.08	8.11	−1.13	−0.81	−5.03
LO	16.71 ± 0.21	2.99	8.08	−1.55*	−0.55	−5.09	−156.33 ± 7.26	−32.83	3.83	−29.53	−39.96	−36.66	8.90 ± 0.21	1.35	8.27	−3.03*	−2.55*	−6.92
MN	12.81 ± 0.38	−0.92	7.08	−5.22*	−3.69*	−8.00	−117.41 ± 2.82	6.10	6.71	7.95	−2.47	−0.61	6.94 ± 0.42	−0.61	7.41	−4.83*	−3.81*	−8.03
MO	16.15 ± 0.23	2.42	7.31	−2.12*	−0.35	−4.89	−112.16 ± 7.89	11.34	5.27	14.63	2.77	6.07	10.54 ± 0.45	2.99	7.58	−1.38	−0.21	−4.58
NO	17.38 ± 0.42	3.66	8.85	−0.88	−0.65	−5.19	−147.47 ± 9.17	−23.96	−5.15	−20.67	−22.11	−18.81	10.01 ± 0.42	2.46	8.59	−1.92	−1.75	−6.13

γ, δ, and w are given as the average plus or minus the standard error over five replicate fitness assay measurements. $\Delta\gamma_{wt}$, $\Delta\delta_{wt}$, and Δw_{wt} denote the fitness effect of the genotype relative to the wild-type (ID8). $\Delta\gamma_{add}$, $\Delta\delta_{ad}$, and Δw_{add} give the expected fitness of a mutation pair under additivity. $\Delta\gamma_1$, $\Delta\delta_1$, and Δw_1 give the effect of adding the first mutation in the double-mutant genotype name into the background of the second, and $\Delta\gamma_2$, $\Delta\delta_2$, and Δw_2 give the effect of the second mutation in the background of the first. These are measurements of sign epistasis. $\epsilon\gamma_{ij}$, $\epsilon\delta_{ij}$, and ϵ_{ij} denote the deviation from additivity, as calculated by Equation 2 or by subtracting the value of $\Delta\gamma_{add}$, $\Delta\delta_{add}$, or Δw_{add} from $\Delta\gamma_{wt}$, $\Delta\delta_{wt}$, or Δw_{wt}. A * for each double-mutant denotes significant sign epistasis for the effects of each single mutation in the background containing the second single mutation.

provided evidence for the additivity of mutational effects with respect to protein stability, and extend this pattern by demonstrating additivity of mutational effects on the stability of an entire viral capsid consisting of many copies of the mutated spike and coat proteins. A similar trend was observed by (Chou *et al.* 2014), who found that beneficial mutations in *Methylobacterium extorquens* were strongly antagonistic with regard to fitness, but interacted additively at the level of enzyme expression. If mutations interact additively with regard to the effects of genotype on phenotype, at least at the simplest phenotypic level, then observed patterns of epistasis must arise from a nonlinear relationship between phenotype and fitness. Interactions between genotype and phenotype are more difficult to model than phenotype–fitness interactions, owing to the relative ease of measuring fitness compared to characterizing its underlying phenotypes (Martin *et al.* 2007; Rokyta *et al.* 2011; Caudle *et al.* 2014). Therefore, if epistasis is arising in the interactions between phenotype and fitness, we have a better chance of understanding, modeling, and predicting it.

Larger effect sizes yield diminishing returns

Within the set of fitness effects for the growth-selection double-mutants and growth effects for the heat-shock and pH-selection double-mutants, the average value of ϵ decreased significantly in correlation with the average expected additive effect ($r^2 = 0.64$; $P < 10^{-7}$; Figure 2). Large differences in deviations from additivity for growth rate were also evident across double-mutant groups (Figure 1A). The average magnitudes of epistasis were −7.23 for fitness among growth-rate double-mutants and −4.85 and −2.68 for growth rate for pH-shock double-mutants and heat-shock double-mutants, respectively, and the average effect sizes for individual mutations were 5.67 for fitness for growth-selection mutants and 3.90 and 2.43 for growth-rate effects for the pH-shock and heat-shock mutants, respectively.

These results provided strong evidence that deviation from additivity on average increases as mutational effect size increases. Rokyta *et al.* (2011) proposed and found empirical evidence for a model of epistasis wherein genotypic effects are additive with regard to phenotype, and epistatic effects on fitness arise from a nonlinear phenotype–fitness map resulting from an intermediate phenotypic optimum. They suggested that most beneficial mutations move a genotype near or beyond this intermediate phenotypic optimum, and that the addition of a second beneficial mutation thus causes negative epistasis. We found support for this hypothesis of an intermediate phenotypic optimum generating fitness-level epistasis in our growth-rate data, as mutational pairs with smaller expected additive fitness effects resulted in significantly smaller magnitudes of ϵ. The linear mapping of genotype onto phenotype is also consistent with our observed epistasis for decay effects. All three of the heat-shock double-mutants that exhibited positive epistasis ($\epsilon > 0$) included mutation I, which was the only heat-shock mutant with a deleterious effect on decay rate. Likewise, all but one of the pH-shock double-mutants that had an $\epsilon > 0$ included at least one mutation with a deleterious effect on

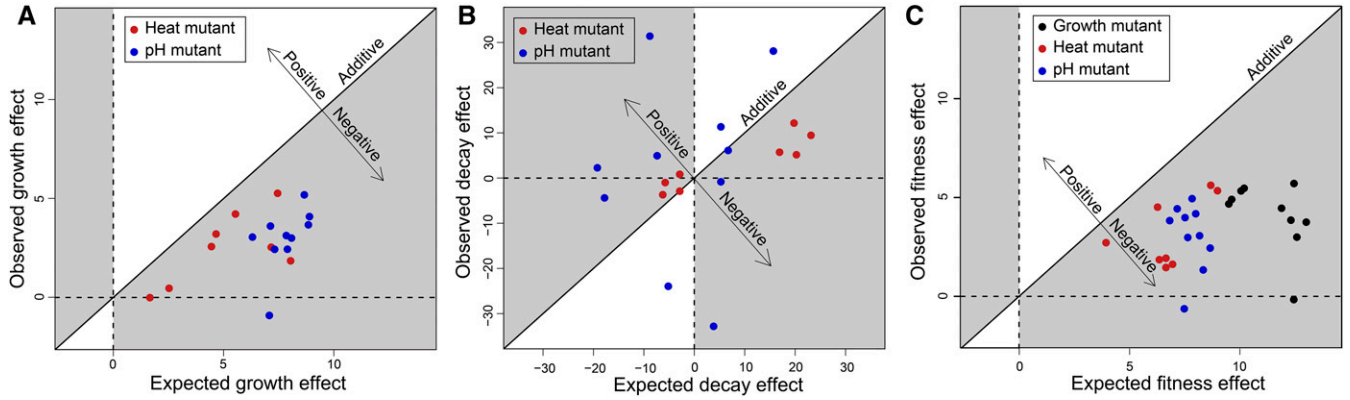

Figure 1 Negative epistasis for growth rate and fitness, but frequent synergism and positive epistasis for decay rate. This figure plots the expected *vs.* observed effects for growth (black), heat-shock (red), and pH-shock (blue) double-mutants. Growth effects (A) and decay effects (B) include all heat-shock and pH-shock double-mutants. Fitness effects (C) include all three sets of double-mutants. Any point falling below the diagonal of additivity is subject to negative magnitude epistasis. Any point above the line indicates positive epistasis. The gray portions of each plot indicate antagonistic epistasis and the white portions synergistic epistasis. Epistasis was universally negative for growth rate and fitness effects, but was frequently positive or nearly additive for decay effects.

decay rate. Combining two beneficial mutations of any effect size led to negative epistasis in all but that one case (GH). In this case, we observed a nonsignificant average deviation from additivity with regard to phenotype (decay rate), but significant and negative epistasis with regard to fitness. The results likewise support similar theoretical predictions of a nonadditive relationship between phenotype and fitness (Martin *et al.* 2007; de Visser *et al.* 2011; Chiu *et al.* 2012).

Recent empirical and theoretical work has shown that there is a distinct upper bound on fitness and that, as populations or genotypes approach this bound, mutational effect size decreases in a pattern of diminishing returns (Rokyta *et al.* 2009; MacLean *et al.* 2010; Chou *et al.* 2011; Kryazhimskiy *et al.* 2014; Schoustra *et al.* 2016). Wang *et al.* (2016) found that the benefit of transferred mutations is better predicted by the fitness of recipients than by their ecological or genetic relatedness, and Kryazhimskiy *et al.* (2014) showed in evolved strains of *Saccharomyces cerevisiae* that although epistasis imposes stochasticity on sequence evolution, fitness evolution tends to follow a predictable trajectory. The preponderance of evidence for diminishing returns of beneficial fitness effects is consistent with results from experimental evolution showing a gradual decline in the rate of fitness increase over the course of an adaptive walk (Lenski *et al.* 1991; Bull *et al.* 1997; de Visser and Lenski 2002; Elena and Lenski 2003; Khan *et al.* 2011). Patterns of diminishing returns are also consistent with recent empirical support for a distribution of beneficial mutational effects characterized by a distinct upper bound on fitness (Rokyta *et al.* 2008; Bataillon *et al.* 2011; Bank *et al.* 2014), such as might arise naturally from an intermediate phenotypic optimum. The increasing magnitude of negative epistasis we observed with an increasing magnitude of individual effects concurs with previous demonstrations of a pattern of diminishing returns, and we extended the characterization of this pattern through our decomposition of fitness into its component phenotypic effects and by pairing mutations covering a wide range of effect sizes for each trait, from highly deleterious to highly beneficial.

Intragenic and deleterious pairings result in sign epistasis

Sign epistasis refers to the form of epistasis wherein the sign of the effect of a particular mutation depends upon its genetic context. This form of epistasis particularly impacts the accessibility of mutational pathways and thus the efficiency and repeatability of adaptive walks (Weinreich *et al.* 2005). Decompensatory epistasis is a particular type of sign epistasis manifested when the effect of a mutation that is beneficial in the wild-type background is deleterious in the presence of a second beneficial mutation.

We analyzed the effect that each mutational pairing had on fitness. In total, of 14 intragenic mutational pairs, 13 had fitness lower than either constituent mutation in the wild-type background, seven significantly so, and nine had fitness significantly lower than at least one of the single mutations (Figure 3;$P < 0.05$ with two-sided Welch's two-sample *t*-tests, Bonferroni corrected for 20 tests). Of 16 intergenic pairs, only four had fitness significantly lower than at least one of their individual mutations (Figure 3, Table 2, Table 3, and Table 4) The magnitude of ϵ relative to the average single-mutant effect size within each selection condition, averaged over all three sets, was -1.49 for intragenic pairings, and only -0.93 for intergenic pairings ($P < 0.0001$ with two-sided Welch's two-sample *t*-tests).

Overall, decompensatory epistasis was observed in nearly all intragenic mutational pairings, and was rarer in intergenic pairs. In cases where fitness of the double-mutant was lower than that of either single-mutant—as with BD, BE, DE, MN, LO, or either of the two lethal heat-shock pairings—the result of epistasis is that there is no viable mutational pathway leading from the wild-type to the double-mutant genotype. In cases where fitness of the double-mutant is intermediate

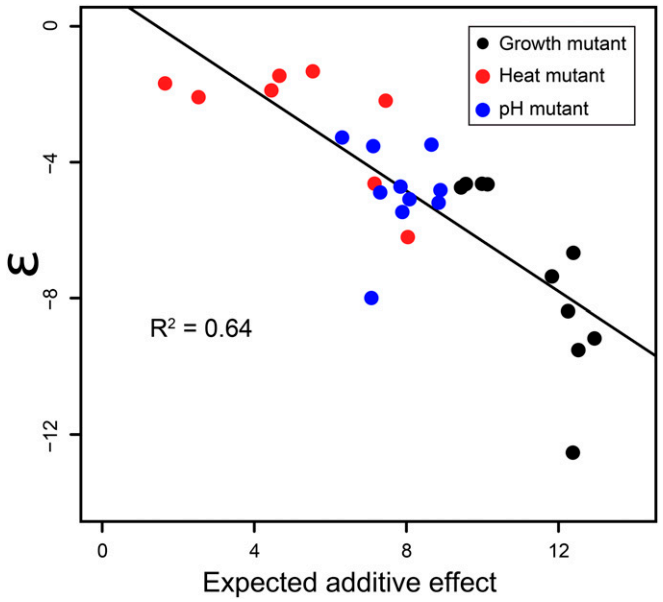

Figure 2 Correlation of growth rate ϵ with expected additive effect size. Combined summary of expected double-mutant effect sizes and corresponding values of ϵ for fitness for all growth-rate (black) double-mutants, and for growth rate for all heat-shock (red) and pH-shock (blue) double-mutants.

to the fitnesses of the single-mutants, as with CE or HI, the order of fixation matters; the sign of the effect of adding the second mutation depends on which mutation was added first.

Another form of sign epistasis, reciprocal sign epistasis, was exhibited by genotype KO. Both K and O were individually deleterious for decay rate, but in combination yielded a double-mutant that was beneficial for decay rate relative to the wild-type (Table 4). In this case, with selection acting only on capsid stability, the only path from the wild-type to the KO genotype would be through simultaneous emergence of K and O on the same background, which is unlikely except in populations of very large size or elevated mutation rate.

Frequent sign epistasis within the sets of intragenic beneficial mutation pairings we explored hinted at a rugged genotype–fitness landscape with many local peaks and valleys, including at least one peak that was inaccessible via single mutational steps. However, the majority of intergenic pairs did not exhibit significant sign epistasis. The overall fitness landscape thus is one of intermediate ruggedness, such that the set of available beneficial mutations may be very different from the first mutational step to the second. The majority of recent empirical evidence indicates that fitness landscapes generally possess an intermediate degree of ruggedness, falling somewhere between a smooth, additive landscape and an uncorrelated, maximally rugged landscape (de Visser and Krug 2014; Neidhard *et al.* 2014; Bank *et al.* 2016), and our results fit with this growing consensus. Additionally, we demonstrated a case where sign epistasis constrained adaptation to a suboptimal peak. A rugged landscape is characterized by many local optima separated by fitness valleys that cannot be crossed via single mutational steps—as in the case of the wild-type genotype and the KO double-mutant—potentially limiting the adaptive potential of populations by causing them to

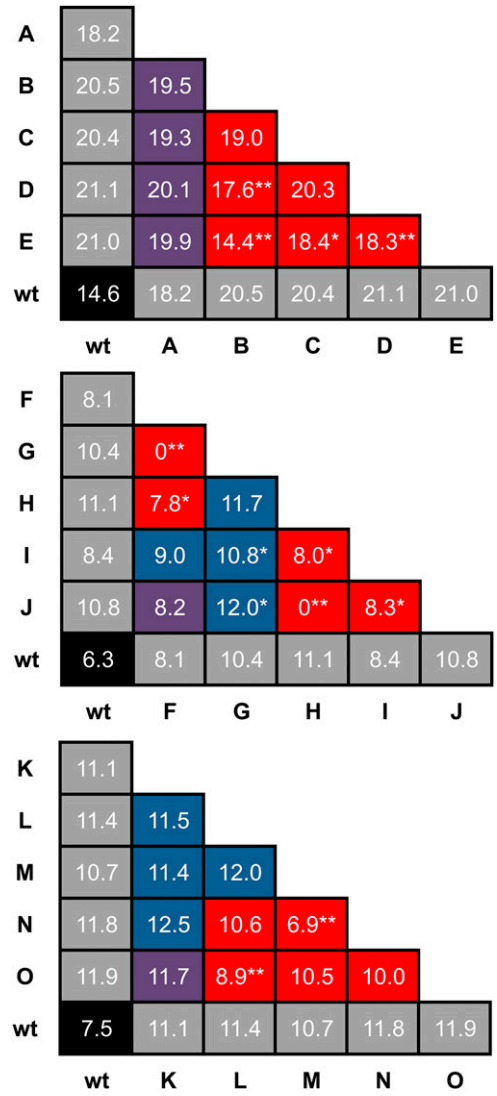

Figure 3 Sign epistasis for fitness is pervasive. A summary of fitness for all mutational pairings. Fitness for each individual mutation is highlighted in gray, wild-type (wt) fitness is shaded in black. Red shading indicates that double-mutant fitness for a given pair was lower than that of either of its constituent mutations, violet indicates fitness between each single-mutant fitness, and blue indicates that the double-mutant exceeded the fitness of either single-mutant. Fitness of 0 is indicated for double-mutants FG and HJ, which were both determined to be lethal pairings. A single * in a red box indicates fitness significantly $<$ 1 for a single-mutant, while ** indicates fitness significantly lower than both singles. A * in a blue box indicates that fitness was significantly higher than both singles. Significance was determined as $P < 0.05$ for a two-sided Welch's two-sample *t*-test, Bonferroni corrected within each set of double-mutants for 20 tests.

become stranded on suboptimal peaks in the landscape (Wright 1932; Kauffman and Levin 1987; Whitlock *et al.* 1995; Neidhard *et al.* 2014).

Antagonistic and sign epistasis in a trio of adjacent substitutions

The effects of combining pairs of mutations from among mutations C, D, and E were particularly interesting in light of their genomic proximity to each other. These mutations are located at

nucleotide positions 4493, 4494, and 4496; C and D affect residue 171 of spike protein G, and E affects residue 172 (Table 1). Both C and D substitute hydrophobic, aliphatic amino acids, alanine and isoleucine, respectively, for a polar threonine residue. C and D in combination substitute valine, a biochemically similar hydrophobic and aliphatic amino acid, for the threonine residue. It is not surprising, then, that CD exhibits fitness indistinguishable from either of the individual effects of C or D (Figure 3 and Table 2), as only one residue is changed, and the change is biochemically similar to the original change of either single mutation. However, the combination of C and E or D and E results in the substitution of two adjacent residues. Both CE and DE have lower fitness than either single-mutant in each pair; CE has fitness significantly lower than E and DE has fitness significantly lower than both D and E ($P < 0.05$ with two-sided Welch's two-sample *t*-tests, Bonferroni corrected for 20 tests).

Although multiple adaptive molecular strategies are available at this region of the spike protein, beneficial mutations within these two residues do not produce additional fitness benefits when present together. The variety of beneficial mutations at these two residues of G led to a high degree of convergent mutation in the original exploration of the first step of adaptation that identified the mutations at residues 171 and 172 (McGee *et al.* 2016). However, the set of beneficial mutations available at the second step of adaptation would not include additional mutations at these sites, indicating that the genotype–fitness map for this region of the spike protein is uncorrelated. Uncorrelated fitness landscapes yield unpredictable adaptation, with the evolutionary trajectories of populations evolving in parallel diverging after the first step in adaptation.

Conclusions

Sign epistasis was prevalent throughout the set of 30 double-mutants, particularly within intragenic pairs of mutations, but not universal, suggesting an intermediate degree of ruggedness within the genotype–fitness landscape. The prevalence of sign epistasis and implied ruggedness of the fitness landscape indicates that the set of available beneficial mutations may be quite different after the first step of adaptation. Our experimentally generated sets of double-mutants universally exhibited negative and antagonistic epistasis with regard to growth rate and fitness, and the magnitude of negative epistasis in growth rate was significantly proportional to the effect size of the individual mutations possessed by each double-mutant. Our results lend support to the increasing evidence that epistasis of fitness effects arises from additive effects of genotype on phenotype and an intermediate phenotypic optimum (Martin *et al.* 2007; de Visser *et al.* 2011; Rokyta *et al.* 2011; Chiu *et al.* 2012; Caudle *et al.* 2014), such that pairs of larger effect beneficial mutations were more likely to overshoot this optimum via additive effects on phenotype, leading to larger magnitudes of negative epistasis.

Patterns of epistasis were more complex for the phenotype of capsid stability, and defy the growing preponderance of evidence for a general trend of negative epistasis between beneficial mutations (Sanjuán *et al.* 2004; Rokyta *et al.* 2011; Caudle *et al.* 2014; Bank *et al.* 2015). Decay rate effects in double-mutants exhibited positive epistasis as often as negative epistasis and an average interaction that was much closer to additivity than for growth rate and fitness when normalized over effect size. The difference in the magnitude of epistasis between growth rate and decay rate effects likely arose from differing scales of phenotypic complexity between the composite phenotype of growth rate and the simple biophysical trait of capsid stability. Our results therefore demonstrated that mutational effects on the underlying components of phenotypes—in this case, the energetics of interaction between capsid subunits—are additive, but epistasis arises in the relationship between phenotype and fitness as a result of interactions between phenotypes and diminishing returns arising from intermediate phenotypic optima.

Acknowledgments

Funding for this work was provided by the U.S. National Institutes of Health to D.R.R. (R01 GM-099723).

Literature Cited

Bank, C., R. T. Hietpas, A. Wong, D. N. Bolon, and J. D. Jensen, 2014 A bayesian MCMC approach to assess the complete distribution of fitness effects of new mutations: uncovering the potential for adaptive walks in challenging environments. Genetics 196: 841–852.

Bank, C., R. T. Hietpas, J. D. Jensen, and D. N. A. Bolon, 2015 A systematic survey of an intragenic epistatic landscape. Mol. Biol. Evol. 32: 229–238.

Bank, C., S. Matuszewski, R. T. Hietpas, and J. D. Jensen, 2016 On the (un)predictability of a large intragenic fitness landscape. Proc. Natl. Acad. Sci. USA 113: 14085–14090.

Bataillon, T., T. Zhang, and R. Kassen, 2011 Cost of adaptation and fitness effects of beneficial mutations in *pseudomonas fluorescens*. Genetics 189: 939–949.

Breen, M. S., C. Kemena, P. K. Vlasov, C. Notredame, and F. A. Kondrashov, 2012 Epistasis as the primary factor in molecular evolution. Nature 490: 535–538.

Bull, J. J., M. R. Badgett, H. A. Wichman, J. P. Huelsenbeck, D. M. Hillis *et al.*, 1997 Exceptional convergent evolution in a virus. Genetics 147: 1497–1507.

Caudle, S. B., C. R. Miller, and D. R. Rokyta, 2014 Environment determines epistatic patterns for a ssDNA virus. Genetics 196: 267–279.

Chiu, H.-C., C. J. Marx, and D. Segré, 2012 Epistasis from functional dependence of fitness on underlying traits. Proc. Biol. Sci. 279: 4156–4164.

Chou, H.-H., H.-C. Chiu, N. F. Delaney, D. Segrè, and C. J. Marx, 2011 Diminishing returns epistasis among beneficial mutations decelerates adaptation. Science 332: 1190–1192.

Chou, H.-H., N. F. Delaney, J. A. Draghi, and C. J. Marx, 2014 Mapping the fitness landscape of gene expression uncovers the cause of antagonism and sign epistasis between adaptive mutations. PLoS Genet. 10: e1004149.

DePristo, M. A., D. M. Weinreich, and D. L. Hartl, 2005 Missense meanderings in sequence space: a biophysical view of protein evolution. Nat. Rev. Genet. 6: 678–687.

Desai, M. S., D. Weissman, and M. W. Feldman, 2007 Evolution can favor antagonistic epistasis. Genetics 177: 1001–1010.

de Visser, J. A. G., and J. Krug, 2014 Empirical fitness landscapes and the predictability of evolution. Nat. Rev. Genet. 15: 480–490.

de Visser, J. A. G., and R. E. Lenski, 2002 Long-term experimental evolution in *Escherichia coli*. XI. rejection of non-transitive interactions as cause of declining rate of adaptation. BMC Evol. Biol. 2: 19.

de Visser, J. A., R. F. Hoekstra, and H. van den Ende, 1997 An experimental test for synergistic epistasis and its application in Chlamydomonas. Genetics 145: 815–819.
de Visser, J. A., T. F. Cooper, and S. F. Elena, 2011 The causes of epistasis. Proc. Biol. Sci. 278: 3617–3624.
Draghi, J. A., and J. B. Plotkin, 2013 Selection biases the prevalence and type of epistasis along adaptive trajectories. Evolution 67: 3120–3131.
Elena, S. F., and R. E. Lenski, 1997 Test of synergistic interactions among deleterious mutations in bacteria. Nature 390: 395–398.
Elena, S. F., and R. E. Lenski, 2003 Evolution experiments with microorganisms: the dynamics and genetic bases of adaptation. Nat. Rev. Genet. 4: 457–469.
Kauffman, S., and S. Levin, 1987 Towards a general theory of adaptive walks on rugged landscapes. J. Theor. Biol. 128: 11–45.
Khan, A. I., D. M. Dinh, D. Schneider, R. E. Lenski, and T. F. Cooper, 2011 Negative epistasis between beneficial mutations in an evolving bacterial population. Science 332: 1193–1196.
Kondrashov, A. S., 1982 Selection against harmful mutations in large sexual and asexual populations. Genet. Res. 40: 325–332.
Kondrashov, A. S., 1988 Deleterious mutations and the evolution of sexual reproduction. Nature 336: 435–440.
Kondrashov, A. S., 1993 Classification of hypotheses on the advantage of ampimixis. J. Hered. 84: 372–387.
Kryazhimskiy, S., D. P. Rice, E. R. Jerison, and M. M. Desai, 2014 Global epistasis makes adaptation predictable despite sequence-level stochasticity. Science 344: 1519–1522.
Kvitek, D. J., and G. Sherlock, 2011 Reciprocal sign epistasis between frequently experimentally evolved adaptive mutations causes a rugged fitness landscape. PLoS Genet. 7: e1002056.
Lehner, B., 2011 Molecular mechanisms of epistasis within and between genes. Trends Genet. 27: 323–331.
Lenski, R. E., M. R. Rose, S. C. Simpson, and S. C. Tadler, 1991 Long-term experimental evolution *Escherichia coli*. I. adaptation and divergence during 2,000 generations. Am. Nat. 138: 1315–1341.
MacLean, R. C., G. G. Perron, and A. Gardner, 2010 Diminishing returns from beneficial mutations and pervasive epistasis shape the fitness landscape for Rifampicin resistance in *pseudomonas aeruginosa*. Genetics 186: 1345–1354.
Martin, G., S. F. Elena, and T. Lenormand, 2007 Distributions of epistasis in microbes fit predictions from a fitness landscape model. Nat. Genet. 39: 555–560.
McGee, L. W., E. W. Aitchison, S. B. Caudle, A. J. Morrison, L. Zheng *et al.*, 2014 Payoffs, not tradeoffs in the adaptation of a virus to ostensibly conflicting selective pressures. PLoS Genet. 10: e1004611.
McGee, L. W., A. M. Sackman, A. J. Morrison, J. Pierce, J. Anisman *et al.*, 2016 Synergistic pleiotropy overrides the costs of complexity in viral adaptation. Genetics 202: 285–295.
Neidhard, J., I. G. Szendro, and J. Krug, 2014 Adaptation in tunably rugged fitness landscapes: the rough Mount Fuji Model. Genetics 198: 699–721.
Olson, C. A., N. C. Wu, and R. Sun, 2014 A comprehensive biophysical description of pairwise epistasis throughout an entire protein domain. Curr. Biol. 24: 2643–2651.
Ono, J., A. C. Gerstein, and S. P. Otto, 2017 Widespread genetic incompatibilities between first-step mutations during parallel adaptation of *saccharomyces cerevisiae* to a common environment. PLoS Biol. 15: e1002591.
Otto, S. P., 2009 The evolutionary enigma of sex. Am. Nat. 174: S1–S14.
Otto, S. P., and M. W. Feldman, 1997 Deleterious mutations, variable epistatic interactions, and the evolution of recombination. Theor. Popul. Biol. 51: 134–147.
Pepin, K. M., and H. A. Wichman, 2007 Variable epistatic effects between mutations at host recognition sites in ϕX174 bacteriophage. Evolution 61: 1710–1724.
Pepin, K. M., M. A. Samuel, and H. A. Wichman, 2006 Variable pleiotropic effects from mutations at the same locus hamper prediction of fitness from a fitness component. Genetics 172: 2047–2056.
Poon, A., and L. Chao, 2005 The rate of compensatory mutation in the DNA bacteriophage phiX174. Genetics 170: 989–999.
Poon, A. F. Y., and L. Chao, 2006 Functional origins of fitness effect-sizes of compensatory mutations in the DNA bacteriophage phiX174. Evolution 60: 2032–2043.
R Development Core Team, 2010 *R: A Language and Environment for Statistical Computing*. R Foundation for Statistical Computing, Vienna, Austria.
Rokyta, D. R., M. R. Badgett, I. J. Molineux, and J. J. Bull, 2002 Experimental genomic evolution: extensive compensation for loss of DNA ligase activity in a virus. Mol. Biol. Evol. 19: 230–238.
Rokyta, D. R., C. Burch, S. B. Caudle, and H. A. Wichman, 2006 Horizontal gene transfer and the evolution of microvirid coliphage genomes. J. Bacteriol. 188: 1134–1142.
Rokyta, D. R., C. J. Beisel, P. Joyce, M. T. Ferris, C. L. Burch *et al.*, 2008 Beneficial fitness effects are not exponential for two viruses. J. Mol. Evol. 67: 368–376.
Rokyta, D. R., Z. Abdo, and H. A. Wichman, 2009 The genetics of adaptation for eight microvirid bacteriophages. J. Mol. Evol. 69: 229–239.
Rokyta, D. R., P. Joyce, S. B. Caudle, C. Miller, C. J. Beisel *et al.*, 2011 Epistasis between beneficial mutations and the phenotype-to-fitness map for a ssDNA virus. PLoS Genet. 7: e1002075.
Sackman, A. M., and D. R. Rokyta, 2013 The adaptive potential of hybridization demonstrated with bacteriophages. J. Mol. Evol. 77: 221–230.
Sackman, A. M., D. Reed, and D. R. Rokyta, 2015 Intergenic incompatibilities reduce fitness in hybrids of extremely closely related bacteriophages. PeerJ 3: e1320.
Sanjuán, R., A. Moya, and S. F. Elena, 2004 The contribution of epistasis to the architecture of fitness in an RNA virus. Proc. Natl. Acad. Sci. USA 101: 15376–15379.
Schoustra, S., S. Hwang, J. Krug, and J. A. G. M. de Visser, 2016 Diminishing-returns epistasis among random beneficial mutations in a multicellular fungus. Proc. Biol. Sci. 283: 20161376.
Vanhaeren, H., N. Gonzalez, F. Coppens, L. D. Milde, T. V. Daele *et al.*, 2014 Combining growth-promoting genes leads to positive epistasis in *Arabidopsis thaliana*. Elife 3: e02252.
Wang, Y., C. D. Arenas, D. M. Stoebel, K. Flynn, E. Knapp *et al.*, 2016 Benefit of transferred mutations is better predicted by the fitness of recipients than by their ecological or genetic relatedness. Proc. Natl. Acad. Sci. USA 113: 5047–5052.
Weinreich, D. M., R. A. Watson, and L. Chao, 2005 Perspective: sign epistasis and genetic constraint on evolutionary trajectories. Evolution 59: 1165–1174.
Wells, J. A., 1990 Additivity of mutational effects in proteins. Biochemistry 29: 8509–8517.
Whitlock, M. C., P. C. Phillips, F. B.-G. Moore, and S. J. Tonsor, 1995 Multiple fitness peaks and epistasis. Annu. Rev. Ecol. Syst. 26: 601–629.
Wright, S., 1932 The roles of mutation, inbreeding, crossbreeding, and selection in evolution. Proceedings of the 6th International Congress of Genetics, Ithaca, New York, Vol. 1, pp. 356–366.
Wright, S., 1988 Surfaces of selective value revisited. Am. Nat. 131: 115–123.
Zee, P. C., and G. J. Velicer, 2017 Parallel emergence of negative epistasis across experimental lineages. Evolution 71: 1088–1095.

Communicating editor: L. Wahl